

Indoor Localization with CSI Fingerprint Utilizing Depthwise Separable Convolution Neural Network

Bo-Yi Chang[†] and Jang-Ping Sheu[‡]

[†]Institute of Communications Engineering, National Tsing Hua University, Taiwan

[‡]Department of Computer Science, National Tsing Hua University, Taiwan

Emails: q4w5e680@gmail.com and sheujp@cs.nthu.edu.tw

Abstract—The WiFi-based localization approach has been widely used in the indoor environment. This paper proposes a Multiple Fingerprints-based Indoor localization system (MIFI). MIFI is based on the depthwise separable convolution neural network technique and utilizes Unmanned Aerial Vehicle (UAV) to help with transmitting fingerprint data. With the help of UAV, human effort can be decreased. In the training phase, we collect the Channel State Information (CSI) of the reference points. In the testing phase, CSI sent at the test locations are collected by Raspberry PI 4 as the input, then the system will output the predicted location. The experiment results show that MIFI can achieve a higher classification accuracy and mean localization distance error than the baseline work. Compared to the CSI data sent from UAV, only a minor performance is lost due to the drift problems of UAV.

Index Terms—Channel State Information, Fingerprint, Indoor Localization, Convolution Neural Networks, Unmanned Aerial Vehicle

I. INTRODUCTION

Location-Based Service (LBS) is one of the most important IoT applications. Though GPS can provide accurate localization results in outdoor environments, indoor environments still cannot get a satisfying result. Thus, finding an alternative approach for the indoor environment is necessary. Some researchers have studied vision-based localization approaches with deep learning. To achieve high localization accuracy with vision data, the authors in [1] and [2] utilize the images obtained by the device's camera and fuse them with other data, such as wireless signals and coarse GPS results, to localize the target. Although these researches can achieve accurate localization results, they usually suffer from the problem of photo quality due to the light condition, camera quality, surroundings, etc. So, the vision-based approaches are not suitable for the indoor environment.

For the Indoor Localization System (ILS), to achieve high accuracy localization, a large number of devices are needed to install in the specified environment. Due to the low cost and convenience, the WiFi-based approach has become the

mainstream of ILS [3] that does not require many additional devices. In the previous ILS research, the Received Signal Strength (RSS) of the wireless signal is widely used in the WiFi-based fingerprint approach [4]. RSS was used as the input, and a database was built to store the fingerprints from various locations. The testing phase matches the fingerprint to the map from the fingerprint database by various approaches, such as the least square approach, maximum likelihood, K-Nearest Neighbors (KNN), and Neural Network (NN) [5], [6]. RSS of the wireless signal is easy to use and widely applied because it can be directly acquired from devices. But RSS is a coarse-grained feature for the indoor environment. The multiple paths and signal blocking problems will severely impact the collected fingerprint data and degrade the relationship between RSS data and location. So, RSS is hard to provide an accurate result.

In contrast with the RSS, Channel State Information (CSI) represents the frequency response of a communication channel, and CSI is a fine-grained feature in the physical layer with higher stability [3], [7]–[10]. However, CSI cannot be directly acquired from most user equipment such as smartphones, and it can be obtained only by modifying the firmware of the specific WiFi network chips [11]–[13]. The CSI extracted from the devices is described in a complex number, which can be transformed into features of Orthogonal Frequency-Division Multiplexing (OFDM) sub-carriers. Compared to RSS, CSI contains features of each sub-carrier, including the phase and the amplitude, which can provide more information than RSS, and it is more stable than RSS. So, we can reach a more accurate result by using CSI over RSS.

Utilize a WiFi-based fingerprint approach to set up ILS need to build a database that stores the fingerprints of all the reference points. But a lot of effort is required to transmit fingerprints by humans, which is time-consuming and labor-consuming. To solve the problem, the authors of [14]–[16] utilize UAV in localization. UAV is helpful with transmitting CSI fingerprints because of its good mobility that can ignore obstacles on the ground and work automatically. With the help of UAV, human work can be significantly reduced.

This paper proposes a multiple Fingerprints-based indoor

This work was supported in part by the Ministry of Science and Technology, Taiwan, under grant MOST 109-2221-E-007-079-MY3 and Qualcomm Technologies, Inc. under grant SOW NAT-435533.

localization system, MIFI, that utilizes human or UAV carrying user equipment (UE) to receive data sent by WiFi AP. As the UE can not acquire CSI directly, we used the Raspberry PI 4 (PI4) as a monitor. PI4 installed the Nexmon framework [13], which uses frame injection to make UE send UDP packets about the information of the physical layer to PI4 after UE received the data transmitted from AP. Then PI4 can extract CSI data from the received UDP packets as the reference data (fingerprints). After preprocessing, the collected CSI data will feed to a depthwise separable convolution neural network. We use the Hampel filter and moving average (MA) filter to reduce the fluctuation of the raw data. We utilize multiple PI4s to collect robust CSI fingerprints for localizing the target. The number of PI4 depends on the size of the environment. More PI4s are needed in a larger area. The experiments show that the localization accuracy of MIFI outperforms the other approaches, such as KNN, XGBoost, Random Forest, and SVM, in indoor environments. In addition, we also show that UAV helps send fingerprint data, reducing human effort and preserving satisfying accuracy compared with data sent manually.

In the remainder of this paper, the system model is presented in Section II. Then, we introduce our scheme in Section III. In Section IV, we provide experimental validation results. Finally, we conclude our work in Section V.

II. SYSTEM MODEL

This section will present the CSI and system model for indoor localization. The CSI consists of the channel characteristics during the signal propagation between the transmitter and receiver, which contains the effects of scattering caused by the surroundings, signal attenuation during propagation, etc. According to IEEE 802.11ac, a signal can be transmitted through sub-carriers with different frequencies and mutually orthogonal by OFDM. Let x_i and y_i denote the transmitted and received signal vectors. We can obtain

$$y_i = Hx_i + N_i, \quad (1)$$

where N_i represents the additive white Gaussian noise. H is the CSI matrix that makes devices adapt transmissions to the channel conditions, which is important to achieve robust communication with high data rates. H can be estimated by x_i and y_i .

Fig. 1 shows the architecture of our system. Our system architecture utilizes multiple PI4s to collect CSI data when the WiFi AP transmits data to the target device, such as a cell phone. The collected CSI fingerprints are stored in a database. After data processing, fingerprints will be input to the machine learning (ML) model. The ML outputs are the probability of the target at different locations where we have collected data. Then, we will use the weighted average to acquire the target's predicted location.

The CSI signal will decrease due to the increased transmitted distance and the signal blocking, multipath propagation, etc. According to [17], the authors have tested how CSI

decrease in a real-world environment. In the real-world environment, PI4 might lose the packets sent by UE, leading to the extracted CSI containing considerable noise in some locations. Therefore, the collected CSI data are not stable enough if we only collect them by one device. So, we use multiple PI4s to collect data that can yield more robust fingerprints than utilizing only one PI4, especially for a large environment. The number of PI4s to collect data depends on the environment's size.

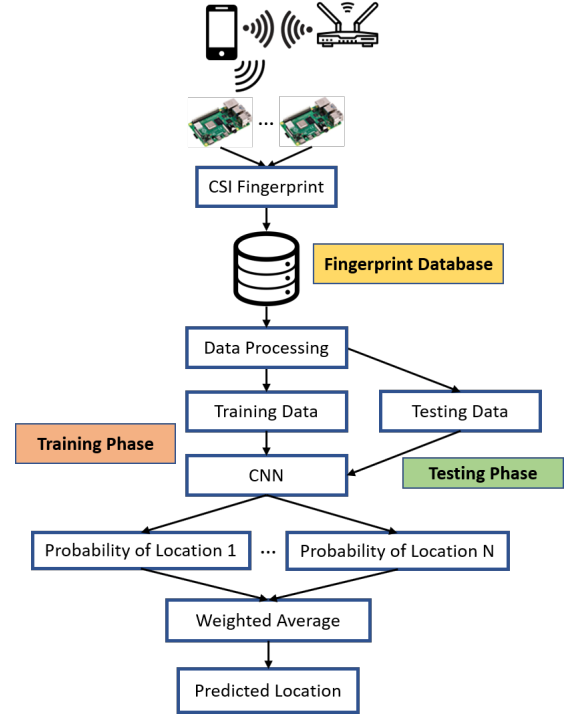


Fig. 1: System Architecture for Multiple PI4s

According to the experiment of the feature selection in [18], the authors assumed the input of the ML model should be the most stable component of the CSI. The stability of CSI is defined as the correlation between the value of CSI collected from a very close location. The experiment tests four components of CSI, including real, imaginary, amplitude (3), and phase (4), respectively. The relationships between the components of CSI are defined as:

$$h = Real + j(Imaginary) \quad (2)$$

$$|h| = \sqrt{(Real)^2 + (Imaginary)^2} \quad (3)$$

$$\angle h = \tan^{-1}\left(\frac{Imaginary}{Real}\right), \quad (4)$$

where $|h|$ is the amplitude of CSI and $\angle h$ is the phase of CSI. The experiment result shows that no matter which sub-carrier is chosen, the correlation of amplitude has the highest stability. The phase component is not stable enough to train a model. So, the amplitude of the CSI is chosen as the input feature of our ML model.

III. MULTIPLE FINGERPRINTS-BASED INDOOR LOCALIZATION SYSTEM (MIFI)

This section will introduce the implementation of our multiple fingerprints-based indoor localization system MIFI, including data preprocessing and ML model algorithm.

A. Data Preprocessing

Though we can acquire the CSI data, the multipath and shadowing will cause the raw data to fluctuate. Therefore, the raw data cannot provide satisfying features for ML if we directly use it as input. So, data preprocessing is necessary for the ML. The raw data collected from the PI4 consist of noise and interference, even if we process it into amplitude. To improve the performance of the CSI data, we need to preprocess the raw input data. Firstly, no matter which bandwidth of WiFi is adopted, null sub-carriers exist that do not transmit data. Secondly, besides the null sub-carriers, pilot sub-carriers are also in the CSI data that do not carry user data. For example, 802.11ac with 80MHz bandwidth, the number of sub-carriers is 256 that ranges from $[-128 \sim 127]$, the usable sub-carriers range from $[-122 \sim -2, 2 \sim 122]$, there are 14 null sub-carriers. The ranges of 8 pilot sub-carriers are $[\pm 11, \pm 39, \pm 75, \pm 103]$. Therefore, 22 sub-carriers should be removed from raw data. Finally, we pick 234 sub-carriers from the original 256 sub-carriers.

After removing the sub-carriers, noise still exists that causes outliers in the CSI data. Here, we utilize a Hampel filter to filter the outliers of the data. For each sample x_i in the vector $V = [x_0, x_1, \dots, x_k]$, where k is the number of receive packets in the specific sub-carrier. The Hampel filter computes the median and the standard deviation of a sliding window W_{hampel} composed of a sample x_i and six surrounding data. If x_i differs from the median by more than three standard deviations, it is replaced with the median. The equation of the Hampel filter is defined as:

$$x_i = \begin{cases} \text{median}, & \text{if } x_i > \text{median} + 3 * \sigma, \\ \text{median}, & \text{if } x_i < \text{median} - 3 * \sigma, \\ x_i, & \text{otherwise,} \end{cases} \quad (5)$$

where σ means the standard deviation. The input of the Hampel filter is consecutive CSI packets from the same sub-carrier, as $[H_{i,j}, H_{i,j+1}, \dots, H_{i,j+(n-1)}]$, where i is one of the 234 sub-carriers after removing the none used ones, j is the packet number, and n is packets we collect at each location. We set $n = 500$ in our experiments.

Although after the Hampel filter, most of the outliers and the noise has been eliminated, there still exists a little noise in the data, causing it is not stable enough to make the ML model learn the characteristic of each location. We utilize the moving average (MA) filter to average the amplitude of consecutive CSI data $[H_{i,j}, H_{i,j+1}, \dots, H_{i,j+n}]$ in the same sub-carrier. The equation of MA is shown below:

$$\text{AverageAmp} = \frac{(\text{Amp}_i + \text{Amp}_{i+1} + \dots + \text{Amp}_{i+(N-1)})}{N}, \quad (6)$$

where N is the window size of each MA filter, i is the number of the continuous CSI amplitude. In our experiment, we pick $N = 3$ to execute the MA filter. After the MA filter, we can get stable fingerprints as the input of MIFI.

B. Machine Learning Model

After data preprocessing, each of the fingerprints contains a 1×234 CSI amplitude matrix, corresponding to the CSI amplitude of 234 sub-carriers. Inspired by MobileNet [19], we designed MIFI based on the depthwise separable convolution that is lighter than traditional convolution and can provide localization results faster. MIFI consists of multiple input layers, each corresponding to a PI4_{*i*} collected by *i*-th PI4. Each input layer follows a series of convolution layers and one fully connected (FC) layer designed with data evaluation. The setting of each layer's parameters is shown in Table I. The series of convolution layers consist of five convolution layers, the first one is a traditional convolution layer, and the others are depthwise separable convolution layers. A concatenate layer concatenates the output of the FC layers from different input layers. Finally, a series of FC layers is set to utilize the concatenate data as input and output the result of the MIFI. After the concatenate layer, the nodes number of the FC layer is set to 64, and SELU is set as the activation function. Then, the number of the output nodes K is dependent on the number of locations stored in the training set. By setting the softmax as the activation function in the output layer, we have the probability of each location in the output of the ML model.

TABLE I: Parameter Setting of Machine Learning Model

Type	Filter Number	Activation Function	Kernel Size	Stride
conv1D	32	SELU	3	2
conv1D dw	32	SELU	3	1
conv1D	64	SELU	1	1
conv1D dw	64	SELU	3	2
conv1D	128	SELU	1	1
AvgPooling	-	-	7	1
Type	Node Number	Activation Function		
Flatten	-	-		
FC	128	SELU		

The localization problem can be assumed as a classification problem that classifies the input data to the location with the highest probability, so we consider category cross-entropy as a loss function to solve the classify function, which is denoted as:

$$\text{Loss} = - \sum_i^C \hat{y}_i \log y_i, \quad (7)$$

where \hat{y}_i is the true value of the target, y_i is the output value of the target, C is the number of categories. Adam optimization is used to optimize the training procedure.

In the training phase, we divide the environment into two-dimensional rectangular grids to determine the target location. Each grid represents a category that MIFI has to learn. The fingerprints collected by different PI4s after finishing preprocessing are used as the training set of MIFI. MIFI will learn the characteristics of the fingerprints collected at each

grid and predict the location of the target. The output of the MIFI is the probability of each grid where the target is.

In the localization phase, its goal is to provide accurate indoor localization service to the users. PI4s collected the CSI data through signals transmitted between AP and UE. Then MIFI utilizes the CSI fingerprints as input and determines the probability of each grid where the target is. However, the user might not be at the location where we have collected data. So, in the localization phase, we pick locations different from the training set as the testing set. For each input from the testing set, we utilize the weighted average approach that picks the top k locations with the highest probability from the output of the model and computes the user's location as follows:

$$\hat{x} = \left(\frac{\sum_{i=1}^k w_i x_i}{\sum_{i=1}^k w_i} \right) \quad (8)$$

$$\hat{y} = \left(\frac{\sum_{i=1}^k w_i y_i}{\sum_{i=1}^k w_i} \right), \quad (9)$$

where \hat{x} and \hat{y} are the user's coordinate in the environment, w_i is the probability of the user in the grid i , and (x_i, y_i) is the coordinate of the grid i . We pick $k = 10$ to compute the predicted location in our experiments. Finally, the mean localization error of the testing set is computed by Root Mean Square Error (RMSE), which is shown below:

$$RMSE = \sqrt{\frac{1}{N} \sum_{i=1}^N (y_i - \hat{y}_i)^2}, \quad (10)$$

where \hat{y} and y are the predicted location and actual location of the testing set, respectively, and N is the number of the testing data.

IV. EXPERIMENTS

To evaluate the performance of our system, we set multiple evaluation cases, including the classification case, localization case, and case of fingerprint data sent from UAV as training input. We will introduce our experiment setup in the following subsection.

A. Experiment Setup

In the following experiments, we use a notebook installed with windows 10 as a WiFi AP, an HTC U12 cell phone as a target device (UE), and two PI4s with kernel version 5.4 and Nexmon framework as monitors to collect the CSI packets when the cell phone is receiving packets from AP. A GPU server with TensorFlow is used to improve the training time. Our devices are running on 802.11ac 80 MHz. A total of 256 sub-carriers can be acquired. We take the amplitude of CSI from the selected 234 sub-carriers as the input of our proposed MIFI model.

In this paper, the real-world indoor localization experiments are in the basement and 7F corridors of the Electrical Engineering and Computer Science (EECS) building in National Tsing Hua University (NTHU) as shown in Fig. 2(a) and Fig. 2(b), respectively. The area size of the basement is $7.15 \text{ m} \times$

3.3 m . The space of 7F corridors consists of two corridors. One is $18.15 \text{ m} \times 1.65 \text{ m}$, and the other is $3.85 \text{ m} \times 1.65 \text{ m}$, respectively. To collect the data, we divide the area into grids. Then we localize the collected data into these grids as the reference points (RPs). RPs in the two regions are divided into two sets, one is for training, and another one is for testing. Training points are marked as blue color, and testing points are marked as red color.

In Fig. 2(a), we divide the area into grids, and the size of each grid is $0.55 \text{ m} \times 0.55 \text{ m}$. We pick 60 grids for training and 18 grids for testing. In Fig. 2(b), the size of each grid is $0.55 \text{ m} \times 0.55 \text{ m}$, and 120 grids are collected in total. We pick 100 grids for training and 20 grids for testing. We collected 500 packets at the center of each grid. MIFI needs only 1.33 seconds to compute 500 packets collected from each PI4 to provide fast localization results to users.

B. Determining the Number of PI4s

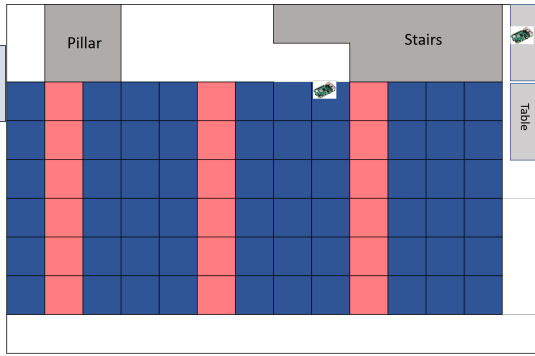
According to our evaluation, the processing time of data collected by one PI4 is 47% of the data using two PI4s. However, the convergence speed of using one PI4 is slower than that of two PI4s and cannot converge to 100% accuracy. This result shows that the data collected by one PI4 cannot provide enough features for machine learning. For the data collected by two PI4s, the accuracy of the validation set can converge to almost 100%. So, we use two sets of CSI data [PI4₁, PI4₂] collected by two PI4s and design MIFI as a two-input model. In addition, combining the characteristics of the fingerprints collected by two PI4s can degrade the ambiguity of the data.

C. Classification and Localization Performance

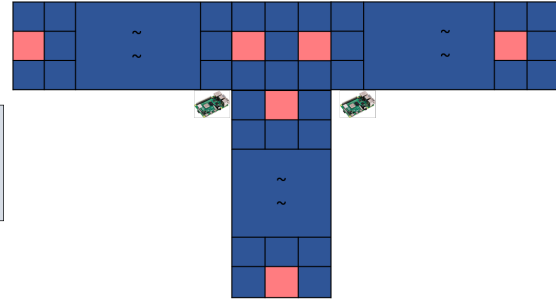
To evaluate the performance of MIFI, we first test with a classification case. We separate the original training set data into 80% of the sub-training set and 20% of the sub-testing set, which means that the locations in the sub-testing set and the sub-training set are the same. This experiment case aims to test whether MIFI can classify the CSI data collected at locations that it has learned.

With the sub-testing set, MIFI can reach 100% accuracy in the basement and corridors of the EECS building, which means that fingerprints at the trained locations have been learned. Compared to other approaches with the same data set, such as KNN, Random Forest, XGBoost, and SVM. The classification results are shown in Table. II. We can observe that MIFI has better classification accuracy than the other models. Though random forest and XGBoost have better performance than KNN and SVM due to the technique of decision trees, all of them cannot process the data with lots of dimensions. So, their classification performance is lower than MIFI.

Secondly, we evaluate the localization ability of MIFI in the basements and corridors. The locations in the training set and the testing set are different. We use the weighted average to get the predicted location of the testing set. The RMSE between the predicted results and true target locations of the basement and corridors are shown in Table III. The MIFI has a 0.90 m



(a) Basement of EECS Building



(b) 7F Corridors of EECS Building

Fig. 2: Experiment Environments

TABLE II: Classification Accuracy

	MIFI	KNN	Random Forest	XGBoost	SVM
Basement of EECS Building					
Grid Size = 0.55 m × 0.55 m	100%	96.85%	98.97%	98.85%	85.04%
Corridors of EECS Building					
Grid Size = 0.55 m × 0.55 m	100%	98.57%	99.7%	99.8%	84.87%

mean error better than KNN, Random Forest, XGBoost, and SVM in the basement case. In the 7F corridors, the MIFI has a 2.28 m mean error between the predicted results and the target's locations, which is better than other approaches in our experiments. The mean error of the corridors is worse than the basement because the area size of the corridor is larger than the basement and the multipath and shadowing of corridors is more affected than the basement. The cumulative distribution function (CDF) of the RMSE results for the basement and corridors are shown in Fig. 3(a) and Fig. 3(b), respectively. The CDF of MIFI is better than other approaches that utilize weighted average to compute predicted location.

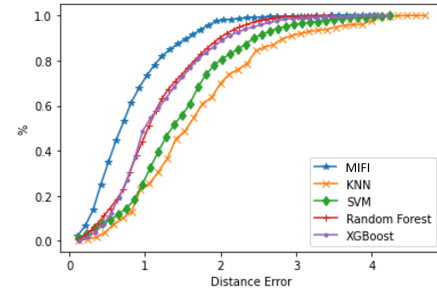
TABLE III: RMSE Results for the Basement and Corridors

	MIFI	KNN	Random Forest	XGBoost	SVM
Basement of EECS Building					
Grid Size = 0.55 m × 0.55 m	0.90 m	1.90 m	1.30 m	1.34 m	1.64 m
Corridors of EECS Building					
Grid Size = 0.55 m × 0.55 m	2.28 m	3.36 m	2.7 m	2.86 m	2.86 m

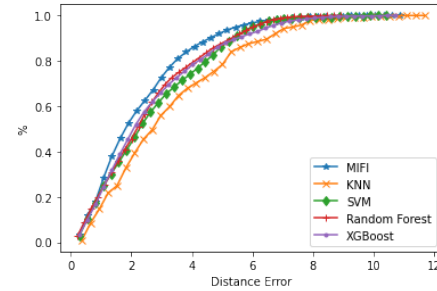
D. Performance Evaluation with Help of UAV

UAVs are helpful for ILS because of their mobility. UAVs usually utilize an ultrasonic sensor to calculate their height. However, it will contain errors due to the height difference and fluctuate collected data. Moreover, in indoor environments, the auto-hover system of the UAV will not work, causing the drift of the UAV's location. So, the ILS with the UAVs must remove the fluctuation of the data and be robust enough to classify the data.

The following experiment is executed in the basement area. To test the performance of MIFI with the help of UAV, we train MIFI with the data sent from the cell phone mounted on



(a) CDF with Grid Size = 0.55 m × 0.55 m in Basement of EECS Building



(b) CDF with Grid Size = 0.55 m × 0.55 m in Corridors of EECS Building

Fig. 3: CDF of Localization Result

the UAV and test with the CSI data sent from the human. The flying height of the UAV is 50 cm ~ 60 cm. Due to the drift problem of UAV, the grid size that we collect data is 1.1 m × 1.1 m, avoiding packets being wrong labeled if the size of the grid is too small. The UAV utilized in our experiment is shown in Fig. 4.

The RMSE of using UAV and human work to send data are shown in Table IV. Due to the ability to process data fluctuation caused by UAV, MIFI outperforms other approaches. For the MIFI scheme, the mean error results of using UAV and human are 1.28 m and 1.09 m, respectively. Compared the localization results that data sent from UAV, with the localization results that data sent from human, a little performance is lost due to the drift problems of UAV. So, utilizing UAV for

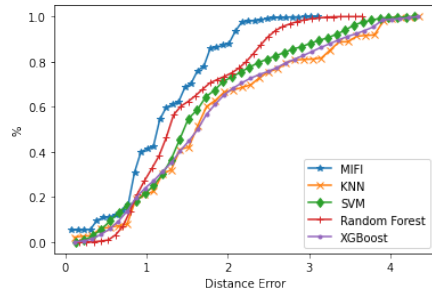


Fig. 4: UAV Photo of Experiment

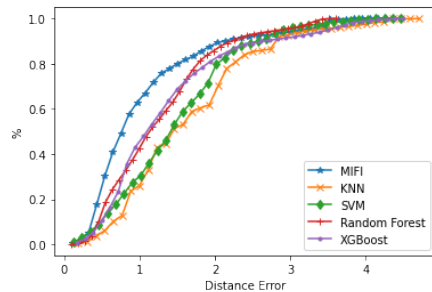
localization can reduce human effort and preserve satisfying localization accuracy in the indoor localization scenario. Fig. 5(a) and Fig. 5(b) show the CDF of the RMSE results for different approaches with the help of UAV and human, respectively. The MIFI is outperforming other methods due to the ability of processing complex data. In addition, the CDF with human help is more stable than the CDF with UAV help.

TABLE IV: RMSE Results with UAV and Human Effort

	MIFI	KNN	Random Forest	XGBoost	SVM
Collect Data with the UAV Help					
Grid Size = 1.1 m × 1.1 m	1.28 m	2 m	1.55 m	1.94 m	1.83 m
Collect Data with the Human Help					
Grid Size = 1.1 m × 1.1 m	1.09 m	1.89 m	1.33 m	1.47 m	1.71 m



(a) CDF with UAV Help in Basement of EECS Building



(b) CDF with Human Help in Basement of EECS Building

Fig. 5: CDF of Localization Results with UAV and Human Effort

V. CONCLUSION

This paper proposes an indoor localization system MIFI based on the depthwise separable convolution layers using CSI fingerprints. Based on our experiments, MIFI utilizes CSI data collected by two PI4s to yield robust fingerprints in our experiment environments. Our model can reduce the computational cost of the network to solve the classification and localization problems. The experiment results show that the locations classification accuracy and mean localization error of MIFI are better than baselines. In addition, with the help of a UAV, the MIFI can reduce human effort significantly and preserve satisfying performance.

REFERENCES

- [1] J. Jiao, F. Li, W. Tang, Z. Deng, and J. Cao, "A hybrid fusion of wireless signals and RGB image for indoor positioning," *International Journal of Distributed Sensor Networks*, vol. 14, no. 2, pp. 1–11, 2018.
- [2] C. Zhang, Y. Duan, J. Xing, and J. Chen, "Deep matching network based image auxiliary localization system for unmanned aerial vehicle," in *IEEE GLOBECOM*, 2019.
- [3] W. Xun, L. Sun, C. Han, Z. Lin, and J. Guo, "Depthwise separable convolution based passive indoor localization using CSI fingerprint," in *IEEE WCNC*, 2020.
- [4] T. Li, W. Wang, and Z. Tu, "Multiple fingerprints-based indoor localization via gbd: Subspace and rssi," *IEEE Access*, vol. 7, pp. 80519 – 80529, 2019.
- [5] C. Own, J. Hou, and W. Tao, "Signal fuse learning method with dual bands WiFi signal measurements in indoor positioning," *IEEE Access*, vol. 7, pp. 131805 – 131817, 2019.
- [6] K. Elawaad, M. Ezzeldin, and M. Torki, "Deepreg: Improving cellular-based outdoor localization using CNN-based regressors," in *IEEE WCNC*, 2020.
- [7] A. Foliadis, M. H. C. Garcia, and R. A. Stirling-Gallacher, "CSI-based localization with CNNs exploiting phase information," in *IEEE WCNC*, 2021.
- [8] Z. Zhou, J. Yu, Z. Yang, and W. Gong, "Mobifi: Fast deep-learning based localization using mobile WiFi," in *IEEE GLOBECOM*, 2020.
- [9] Y. Zhao, W. Wong, H. K. Garg, T. Feng, Z. Zhang, and L. Tang, "Indoor position recognition and interference classification with a nested LSTM network," in *IEEE GLOBECOM*, 2019.
- [10] L. Chen, I. Ahriz, and D. L. Ruyet, "CSI-Based probabilistic indoor position determination: An entropy solution," *IEEE Access*, vol. 7, pp. 170048 – 170061, 2019.
- [11] D. Halperin, W. Hu, A. Sheth, and D. Wetherall, "Tool release: gathering 802.11n traces with channel state information," *ACM SIGCOMM Computer Communication Review*, vol. 41, p. 53, 2011.
- [12] Y. Xie, Z. Li, and M. Li, "Precise power delay profiling with commodity WiFi," *IEEE Transactions on Mobile Computing*, vol. 18, pp. 1342 – 1355, 2019.
- [13] F. Gringoli, M. Schulz, J. Link, and M. Hollick, "Free your CSI: A channel state information extraction platform for modern WiFi chipsets," in *ACM Workshop on Wireless Network*, 2019.
- [14] G. Wu, "UAV-Based interference source localization: A multimodal Q-Learning approach," *IEEE Access*, vol. 7, pp. 2169–3536, 2019.
- [15] S. Piao, Z. Ba, L. Su, D. Koutsonikolas, S. Li, and K. Ren, "Automating CSI measurement with UAVs: from problem formulation to energy-optimal solution," in *IEEE INFOCOM*, 2019.
- [16] P.-Y. Hong, C.-Y. Li, H.-R. Chang, Y. Hsueh, and K. Wang, "WBF-PS: WiGig beam fingerprinting for UAV positioning system in GPS-denied environments," in *IEEE INFOCOM*, 2020.
- [17] H. Zhang, H. Du, Q. Ye, and C. Liu, "Utilizing CSI and RSSI to achieve high-precision outdoor positioning: A deep learning approach," in *IEEE ICC*, 2019.
- [18] A. Sobehy, E. Renault, and P. Muhlethaler, "CSI-MIMO: K-nearest Neighbor applied to indoor localization," in *IEEE ICC*, 2020.
- [19] A. G. Howard, M. Zhu, B. Chen, D. Kalenichenko, W. Wang, T. Weyand, M. Andreetto, and H. Adam, "Mobilenets: Efficient convolutional neural networks for mobile vision applications," *arXiv:1704.04861*, 2017.